

## Calibration of a new very large eddy simulation (VLES) methodology for turbulent flow simulation

HAN XingSi<sup>1\*</sup>, YE TaoHong<sup>2</sup> & CHEN YiLiang<sup>2</sup>

<sup>1</sup>Division of Fluid Dynamics, Department of Applied Mechanics, Chalmers University of Technology, Gothenburg SE-41296, Sweden;

<sup>2</sup>Department of Thermal Science and Energy Engineering, University of Science and Technology of China, Hefei 230027, China

Received August 9, 2011; accepted February 20, 2012; published online August 23, 2012

Following the idea of Speziale's Very Large Eddy Simulation (VLES) method, a new unified hybrid simulation approach was proposed which can change seamlessly from RANS (Reynolds-Averaged Navier-Stokes) to LES (Large Eddy Simulation) method depending on the numerical resolution. The model constants were calibrated in accordance with other hybrid methods. Besides being able to approach the two limits of RANS and LES, the new model also provides a proper VLES mode between the two limits, and thus can be used for a wide range of mesh resolutions. Also RANS simulation can be recovered near the wall which is similar to the Detached Eddy Simulation (DES) concept. This new methodology was implemented into Wilcox's  $k-\omega$  model and applications were conducted for fully developed turbulent channel flow at  $Re_\tau = 395$  and turbulent flow past a square cylinder at  $Re = 22000$ . Results were compared with LES predictions and other studies. The new method is found to be quite efficient in resolving large flow structures, and can predict satisfactory results on relative coarse mesh.

**hybrid RANS-LES method, Very Large Eddy Simulation (VLES), channel flow, flow past a square cylinder**

**PACS number(s):** 47.27.Ak, 47.27.ep, 47.27.em, 47.27.nd, 47.27.wb

**Citation:** Han X S, Ye T H, Chen Y L. Calibration of a new very large eddy simulation (VLES) methodology for turbulent flow simulation. *Sci China-Phys Mech Astron*, 2012, 55: 1905–1914, doi: 10.1007/s11433-012-4886-3

### 1 Introduction

In many industrial and engineering applications, the RANS approach is still the dominant method to simulate turbulent flows at the high Reynolds number. However, the RANS method performs poorly in complex unsteady flows which are dominated by coherent large-eddy structures. LES can resolve the large structures accurately as the unsteady large-scale turbulent motions are explicitly resolved in LES mode. Unfortunately, LES is often not computationally feasible, as it suffers from a very restrictive grid resolution requirement near the wall. An idea, namely hybrid RANS-LES methodology, pursued by many researchers is to switch to or gradually blend to a RANS method near the wall. The concept underlying is to combine the computational efficiency of RANS for modeling the flow in the near-wall regions, with the accurate

LES method to simulate the large-scale turbulent structures in the regions away from the wall. DES method [1] is the most popular one of such hybrid methods and has been used in the studies of many complex flow problems [2–5]. The concept of DES implies that the LES method is used in the region away from the wall, and thus the mesh resolution in this region should be fine enough in order to perform a LES calculation. Unfortunately, the LES still requires much computation cost even for wall-free turbulent flows at the high Reynolds number. It is therefore not easy to afford the cost to perform a real DES for those flows at the high Reynolds number in engineering flow problems.

Alternatively, there is another kind of hybrid methodology, namely VLES, which was firstly proposed by Speziale [6]. This approach was later called Flow Simulation Methodology (FSM) [7] and has shown efficiency and robustness in some applications. In this approach, a generalized turbulence model is obtained by rescaling a conventional RANS model

\*Corresponding author (email: xingsi@chalmers.se)

through the introduction of a resolution control function  $F_r$ , i.e. the subscale turbulent stress tensor is modeled by damping the Reynolds stresses, that is  $\tau_{ij}^{sub} = F_r \tau_{ij}^{RANS}$ , in which the resolution control function  $F_r$  is the core of the VLES modeling. For the original VLES model proposed by Speziale [6], the  $F_r$  was designed to be a function involving two turbulence length scales, in the form of

$$F_r = \left[ 1.0 - \exp(-\beta \Delta / L_k) \right]^n, \quad (1)$$

where  $\beta \sim O(10^{-3})$  and  $n \sim O(1)$  are some modeling parameters which are not specified by Speziale,  $\Delta$  is the representative mesh spacing (cutoff length scale), and  $L_k$  is the Kolmogorov length scale defined as  $L_k = \nu^{3/4} / \varepsilon^{1/4}$ . In the limit as  $\Delta / L_k \rightarrow 0$ , all relevant scales are resolved (e.g.  $\tau_{ij}^{sub} = 0$ ), i.e. the model approaches a DNS method. The regular RANS behavior is recovered (e.g.  $\tau_{ij}^{sub} = \tau_{ij}^{RANS}$ ) at the other limit as  $\Delta / L_k \rightarrow \infty$  as the mesh becomes coarse. The most important feature of this method is that there is a smooth transition from the limit of RANS to DNS and it is considered as a VLES mode between the two limits, which means that when the numerical resolution is not fine enough to resolve the “full range” turbulent scales, it is able to resolve the “very large eddies” to account for their non-linear interaction with the mean flow.

However, the model damps the Reynolds stress too much, nearly impossible to recover to a RANS simulation unless the mesh is unreasonably coarse [8]. Therefore, the model needs quite fine mesh resolutions near the wall like a LES method and doesn't work efficiently for wall-bounded flows. Furthermore, there are a number of issues which were never completely specified by Speziale (please refer to [9]). The important one is that properly reaching both the DNS and RANS limits in this model doesn't guarantee the corresponding approach provides a correct LES mode. As pointed out by Sagaut et al. [9] when the Reynolds number tends to infinity (i.e.  $L_k \rightarrow 0$ ), this model systematically gives a RANS behavior according to eq. (1), which means that the grid spacing has no influence anymore on the eddy viscosity and an LES subgrid scale cannot be reached as fine as the grid is. Considering these, we proposed a variant of the VLES model [10] by replacing the reference length scale from Kolmogorov length scale  $L_k$  to  $L_{RANS}$ , where  $L_{RANS}$  is the integral length scale in a RANS sense, which has the form of

$$F_r = \left[ 1.0 - \exp(-\beta \Delta / L_{RANS}) \right]^n \quad \text{with} \quad L_{RANS} = k^{3/2} / \varepsilon, \quad (2)$$

where  $\beta \sim O(1)$  and  $n \sim O(1)$  are some modeling parameters. However, the two model constants were not specified in our previous study [10]. Consequently, the present study tried to calibrate the two model constants and thus build a sophisticated VLES model for general flow studies. The new model's performance is validated in the applications for two classical flows, the fully-developed turbulent channel flow and turbulent flow past a square cylinder at  $Re = 22000$ .

## 2 Mathematical formulation

There are several other approaches following the idea of VLES model, such as the Limited Numerical Scales (LNS) approach by Batten et al. [11], the Partially Resolved Numerical Simulation (PRNS) by Liu and Shih [12], and a newly developed approach by Hsieh et al. [13]. In the present paper, the acronym VLES is used to refer generically to all these similar strategies. For these strategies, the core of the VLES model is the form of the resolution control function  $F_r$  which affects the simulation significantly especially when the numerical resolution is coarse. Here, we start with the proposed form as shown in eq. (2). In the limit of very fine mesh resolution, it can be got from eq. (2) by using the Taylor expansion

$$F_r \rightarrow \left[ \frac{\beta \Delta}{L_{RANS}} \right]^n \quad \text{with} \quad \Delta \rightarrow 0. \quad (3)$$

Meanwhile, the VLES should approach an LES model in this limit. It can be seen that eq. (3) has exactly the same form as in the analysis by Sagaut et al. [9], which implies that the new VLES model can approach a classical LES model in the limit of very fine mesh resolution. Compared with eq. (3) and the results in ref. [9], we can calibrate the model constant  $n$  as  $n = 4/3$ . However, there is also a same formula proposed by Peltier and Zajackowski [14], which has a different model constant of  $n$ , i.e.  $n = 2$ . Consistent with these studies, the model constant  $n$  can be calibrated as:

$$n = 4/3 \quad \text{or} \quad n = 2. \quad (4)$$

In the following, it will be referred to as  $n1 = 4/3$  and  $n2 = 2$ .

To calibrate the model constant  $\beta$ , we follow the idea by Johansen et al. [15] who assumed that the standard  $k-\varepsilon$  model becomes identical to the Smagorinsky LES model when  $\beta \Delta = L_{RANS}$ . In this situation, the model constant  $\beta$  is related to the Smagorinsky LES model constant  $C_s$  in the form of (refer to [15])

$$\beta = \sqrt{0.3} C_s / C_\mu, \quad (5)$$

where  $C_\mu = 0.09$  is the model constant in the standard  $k-\varepsilon$  model. As the typical Smagorinsky model constant  $C_s$  has a value of 0.1, we can get the model constant  $\beta$

$$\beta = \sqrt{0.3} C_s / C_\mu = 0.61 \quad \text{with} \quad C_s = 0.1. \quad (6)$$

Based on the analysis above, the model constants  $n$  and  $\beta$  in eq. (2) are calibrated and have fixed values, which are also consistent with previous studies. Consequently, the proposed model shown in eq. (2) is established in a complete form.

In practice, the VLES model can be implemented on the basis of several RANS turbulence models, such as standard  $k-\varepsilon$  model,  $k-\omega$  model, etc. Here, we prefer to use Wilcox's  $k-\omega$  model [16] as it has been successfully used in a wide range of flow problems. There are also several different approaches to achieve the VLES modeling based on the RANS model [11–13], and a simple one is adopted in the present

study as used in [11,12], i.e. the governing equations of the VLES model are unchanged as in the original RANS model and only the formula of the turbulent viscosity is scaled with the resolution control function  $F_r$ . For the present implementation based on Wilcox's  $k-\omega$  model, the modeled transport equations for  $k$  and  $\omega$  are exactly the same as in the original Wilcox's  $k-\omega$  model, given by

$$\frac{D\rho k}{Dt} = P_k - \rho\beta_0^* f_{\beta^*} k\omega + \frac{\partial}{\partial x_j} \left[ \left( \mu + \frac{\mu_t}{\sigma_k} \right) \frac{\partial k}{\partial x_j} \right], \quad (7)$$

$$\frac{D\rho\omega}{Dt} = \alpha \frac{\omega}{k} P_k - \rho\beta_0 f_{\beta} \omega^2 + \frac{\partial}{\partial x_j} \left[ \left( \mu + \frac{\mu_t}{\sigma_\omega} \right) \frac{\partial \omega}{\partial x_j} \right]. \quad (8)$$

However, the formula of the turbulent viscosity is changed with the inclusion of  $F_r$ , i.e.

$$\mu_t = F_r \rho k / \omega, \quad (9)$$

where the  $F_r$  is shown in eq. (2). Note that in the framework of  $k-\omega$  model, the length scales in eq. (2) are calculated as:

$$\Delta = (\Delta_x \Delta_y \Delta_z)^{1/3}, \quad L_{RANS} = k^{3/2} / \varepsilon \quad \text{with} \quad \varepsilon = 0.09 k \omega. \quad (10)$$

The model constants  $n$  and  $\beta$  in eq. (2) are given in eqs. (4) and (6), respectively. The other model constants in eqs. (7) and (8) are exactly the same as in the original Wilcox's  $k-\omega$  model (refer to [16] for details).

It should be noted from eq. (2) that, when the mesh resolution is coarse,  $F_r \rightarrow 1$  and the VLES approaches a RANS simulation, and when the mesh is fine enough,  $F_r$  has the form as in eq. (3) and an LES approach is recovered. Between the two limits, the  $F_r$  has a value between 0 and 1 and provides a VLES model. Near the wall, as the integral length scale  $L_{RANS}$  is very small, then  $F_r \rightarrow 1$  and the RANS simulation is recovered, which is similar to the DES concept.

### 3 Numerical details

The new VLES model was implemented in a finite-volume method CFD code. The convective terms are discretized using a second-order central differencing scheme for channel flow and a bounded central differencing scheme for the flow past a square cylinder. The second-order upwind scheme was used for turbulence model governing equations. The temporal advancement was approximated using a second-order implicit scheme. SIMPLEC algorithm was used for pressure-velocity coupling.

## 4 Results and discussion

### 4.1 Turbulent channel flow at $Re_\tau = 395$

The test case is selected to highlight the feasibility of the new VLES model in computations of the attached boundary layer flows. The DNS of Moser et al. [17] for a fully-developed

turbulent channel flow at  $Re_\tau = 395$ , based on the friction velocity  $u_\tau$  and half of the channel height,  $\delta = L_y/2$ , was taken as the benchmark test case. The computational domain has a physical extent of  $L_x = 3.2$ ,  $L_y = 2.0$  and  $L_z = 1.6$  [18] in the streamwise ( $x$ ), wall-normal ( $y$ ) and spanwise ( $z$ ) directions, respectively. A  $32 \times 64 \times 32$  mesh has been used in the  $x$ ,  $y$ , and  $z$  directions, respectively. The mesh is clustered near the wall and the first cell center is located at  $y^+ \approx 1.0$ . For reference, the Smagorinsky LES model [19] was also employed in this computation. Mass flow rate was imposed at the inlet according to the DNS study in ref. [17], and periodic boundary conditions were used in both of the streamwise and spanwise directions. The time-averaged flow fields were obtained by the average process for at least 200 channel flow time, and they were also averaged in both of the streamwise and spanwise directions.

The predictions of friction velocity by different models are compared in Table 1, where "VLES-n1" refers to the present VLES model using a model constant of  $n = 4/3$ , "VLES-n2" refers to the VLES model using  $n = 2$ , in eq. (2), and "LES" refers to the Smagorinsky LES model. It can be seen that the present VLES models predict satisfactory results on this coarse mesh, and better than the result of LES model compared with DNS. Furthermore, the result of VLES-n1 model is closer than the VLES-n2 model to DNS prediction. Figure 1 shows the predicted isosurfaces of the steamwise vorticity  $\omega_x$  by different models. Large flow structures are all recovered by the three models. However, there are obvious differences in the regions near the wall, i.e. the present VLES models predict more and smaller flow structures than the LES model. Furthermore, the VLES-n1 model resolved smaller flow structures than the VLES-n2 model, which implies that the VLES-n1 model is more efficient in resolving the flow structure on the same mesh. This corresponds to the observation in Table 1 that the VLES-n1 model predicts better results than the VLES-n2 model.

Figure 2 compares the computed velocities using different models. Note that the velocities are all nondimensionalized with their individual computed friction velocity  $u_\tau$  shown in Table 1. For the mean streamwise velocity, the present VLES models give much better results than the LES model, and also the results agree with DNS well considering that the mesh is quite coarse. The viscous sublayer and the buffer layer near the wall are accurately resolved, and the log-law region is also resolved well except in the central region of the channel. Due to the two VLES models, they give quite close results. Similar results are also observed in the RMS velocity comparisons. The VLES models predict better results than LES for the RMS velocities in all the three directions. The strong anisotropy of the RMS velocities is also reasonably captured compared with the DNS results.

**Table 1** Computed friction velocity  $u_\tau$  by different models

	DNS [17]	VLES-n1	VLES-n2	LES
$u_\tau$	1.0	1.052	1.074	1.222

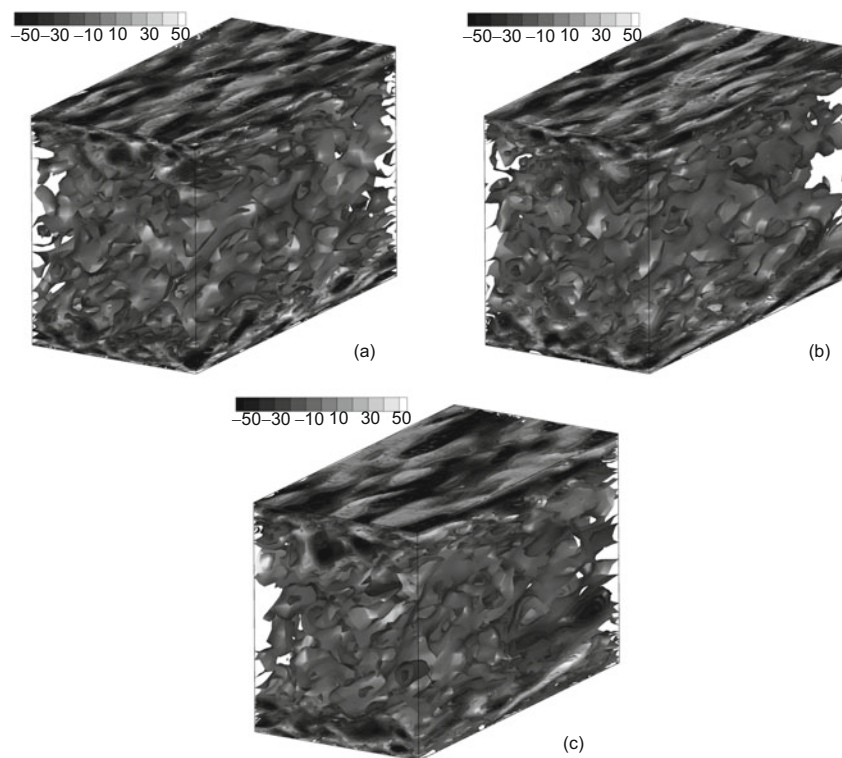


**Figure 1** Isosurfaces of the computed streamwise vorticity  $\omega_x$  by different models. (a) VLES-n1 model; (b) VLES-n2 model; (c) LES model.

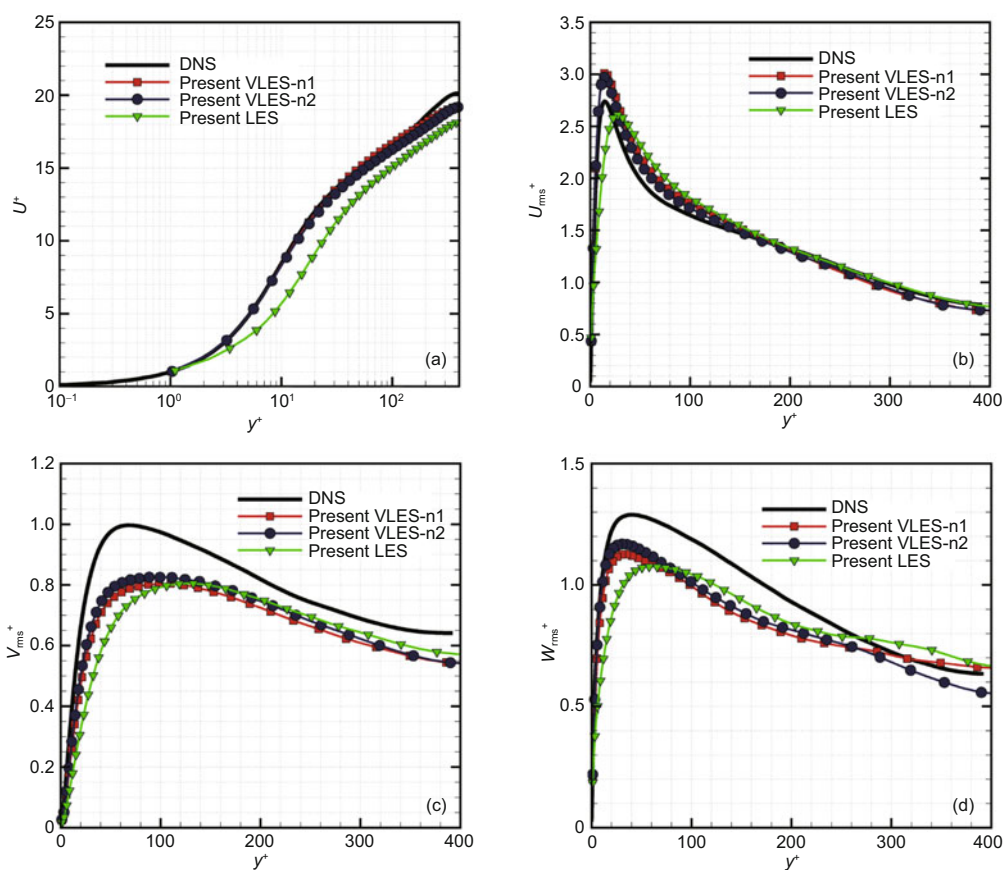


**Figure 2** (Color online) Distributions of averaged velocities. (a) Streamwise velocity; (b) RMS velocity in the  $x$  direction; (c) RMS velocity in the  $y$  direction; (d) RMS velocity in the  $z$  direction.

The results for the channel flow demonstrate that the present VLES models are quite efficient in resolving the turbulent flow structures near the wall, even on the coarse mesh. Better results were obtained than Smagorinsky LES model. Overall, the VLES-n1 model and VLES-n2 model give quite close results, but the VLES-n1 is slightly superior to the VLES-n2 model as demonstrated in Table 1, Figure 1 and Figure 2.

#### 4.2 Flow past a square cylinder at $Re = 22000$

The new VLES model is also applied for the flow past a square cylinder at  $Re = 22000$  based on the cylinder edge length  $D$ . The square cylinder is aligned in the  $z$  (spanwise) direction and the inlet flow is set in the  $x$  (streamwise) direction. The computational domain has a physical extent of  $20D \times 14D \times 4D$ . The lateral dimension  $14D$  is the same as in Lyn's experiment [20], and the lateral boundaries are also subject to the wall boundary conditions consistent with experiment. Two different coarse meshes are used. The grid is clustered near the wall and the first node is located around  $y^+ = 1.0$ . The first mesh (referred to as "mesh1") is quite coarse with a resolution of about 0.191 million cells, and the second one (refers to "mesh2") is by fining the first mesh near the square cylinder (within  $2.0D$ ) resulting in a mesh containing about 0.495 million cells, which is actually quite coarse too, compared with the LES studies by Sohankar and Davidson [21] using a mesh of about 1.066 million cells, and the DES studies by Barone and Roy [2] using a mesh with 8.467 million cells. The flow was simulated by both the VLES-n1 model and VLES-n2 model on the two sets of mesh.

The global parameters of the flow fields are compared in Table 2 against some previous studies. Although both meshes used are very coarse compared with previous numerical studies, all the global parameters predicted are acceptable. On the finer mesh, the results of these global parameters are not improved obviously. However, from another point of view, it shows that the present VLES model can predict quite reasonable results on very coarse mesh such as the first set of mesh (with 0.191 million cells). As the DES study in ref. [2] used a very fine mesh (8.467 million cells), their results are more suitable for the reference evaluating the results of the present VLES models. Overall, the VLES models underpredict the Strouhal number about 2.0%, overpredict the mean drag coefficient about 7.9%, underpredict the RMS drag coefficient

about 20.1% and overpredict the RMS lift coefficient about 15.1%. There are larger differences in the RMS drag and lift coefficient results. However, if the results are compared with the experimental results in ref. [23], the comparison results will be changed obviously. Considering that there exist big differences between the results of previous different studies, the predictions of present VLES model are acceptable. Besides, previous DES studies [2] also found that the Strouhal number becomes smaller, the RMS drag coefficient becomes smaller and the RMS lift coefficient becomes larger with decreasing the mesh resolution. Actually, the results of present VLES model are more close to those by DES study in ref. [2] on the medium mesh (about 2.508 million cells).

Figure 3 shows the predicted isosurfaces of the spanwise vorticity  $\omega_z$  by the two VLES models on two meshes. The four simulations all recover the complex flow structures. The vortex shedding phenomenon is clearly visible in all the plots. Note that the four plots are not at the same phase of the vortex shedding. The results demonstrate that the present VLES model can resolve the "very large eddies" in this flow field. Figure 4 shows the predicted flow fields of the averaged velocities in the middle plane by VLES-n1 model on mesh2. As the other three simulations give similar results, they are not shown here. The results demonstrate that the mean flow structures are well recovered compared with many previous studies, such as in refs. [2,21]. It implies that although the "very large eddies" have complex nonlinear interactions, the present VLES models can provide a proper mode modeling the interactions, and thus the mean flow fields and the RMS flow fields can be recovered reasonably.

Figure 6 shows the averaged streamwise velocity along the central line in the middle plane by the present VLES model along with the results of LES dynamic Smagorinsky model in ref. [21] and DES model in ref. [2]. Predictions by the present VLES model in the near-wake are quite close to each other in the four simulations. Further downstream, the VLES models overpredict the level of wake recovery. Overall, the VLES models predict obvious better results than the LES study in ref. [21], while still have obvious differences compared with the DES study in ref. [2] with a fine mesh and experimental results in ref. [20]. Note that it is quite hard to exactly predict the wake recovery and many previous studies overpredicted the wake recovery compared with the experimental result in ref. [20]. Actually, the present VLES results are quite close the result by DES study in ref. [2] on the

**Table 2** Comparisons of global flow parameters between different models

	$Re/10^3$	$St$	$C_{D,mean}$	$C_{D,RMS}$	$C_{L,RMS}$
VLES-n1-mesh1	22	0.123	2.29	0.22	1.38
VLES-n2-mesh1	22	0.123	2.29	0.19	1.33
VLES-n1-mesh2	22	0.122	2.27	0.22	1.31
VLES-n2-mesh2	22	0.122	2.26	0.20	1.32
LES [21]	22	0.126–0.132	2.03–2.32	0.16–0.20	1.23–1.54
DES (fine) [2]	19.4	0.125	2.11	0.26	1.16
Exp. Lyn [20]	21.4	0.132	2.1	-	-
Exp. Durao [22]	14	0.138	-	-	-
Exp. Luo [23]	34	0.13	2.2	0.18	1.2

medium mesh with about 2.508 million cells (not shown here).

Figure 5 shows the RMS velocities along the central line in the middle plane by the present VLES models along with

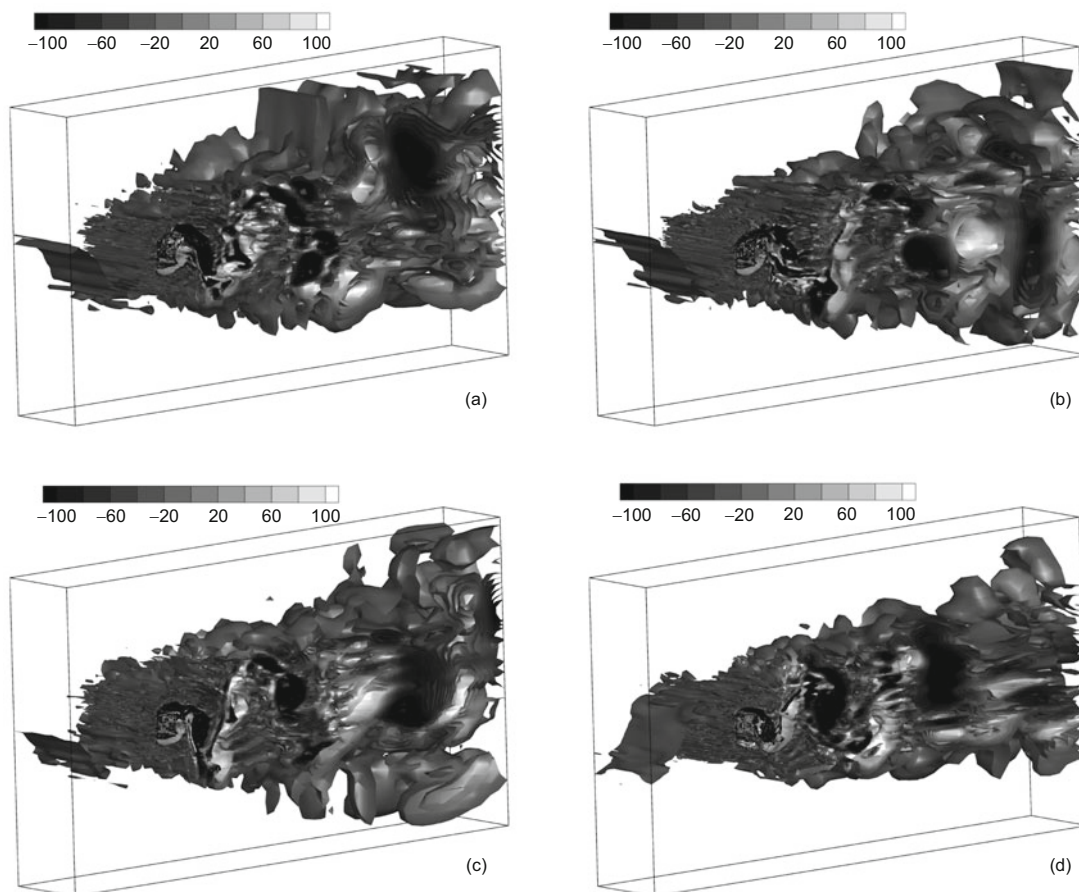


**Figure 3** Isosurfaces of the computed spanwise vorticity  $\omega_z$ . (a) VLES-n1 model on mesh1; (b) VLES-n2 model on mesh1; (c) VLES-n1 model on mesh2; (d) VLES-n2 model on mesh2.

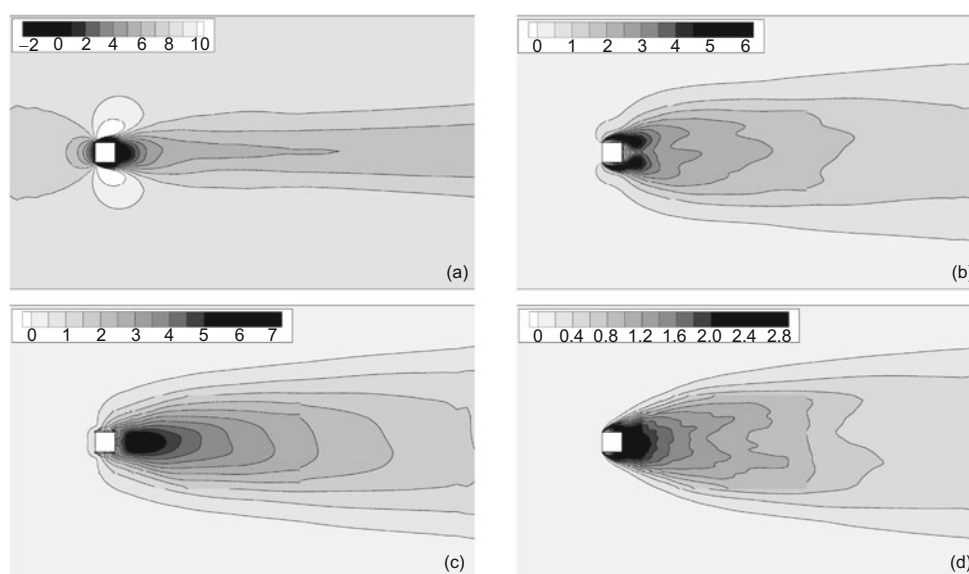


**Figure 4** Averaged velocity flow field in the middle plane by VLES-n1 model on mesh2. (a) Mean streamwise velocity  $U$ ; (b) RMS velocity in the  $x$  direction; (c) RMS velocity in the  $y$  direction; (d) RMS velocity in the  $z$  direction.

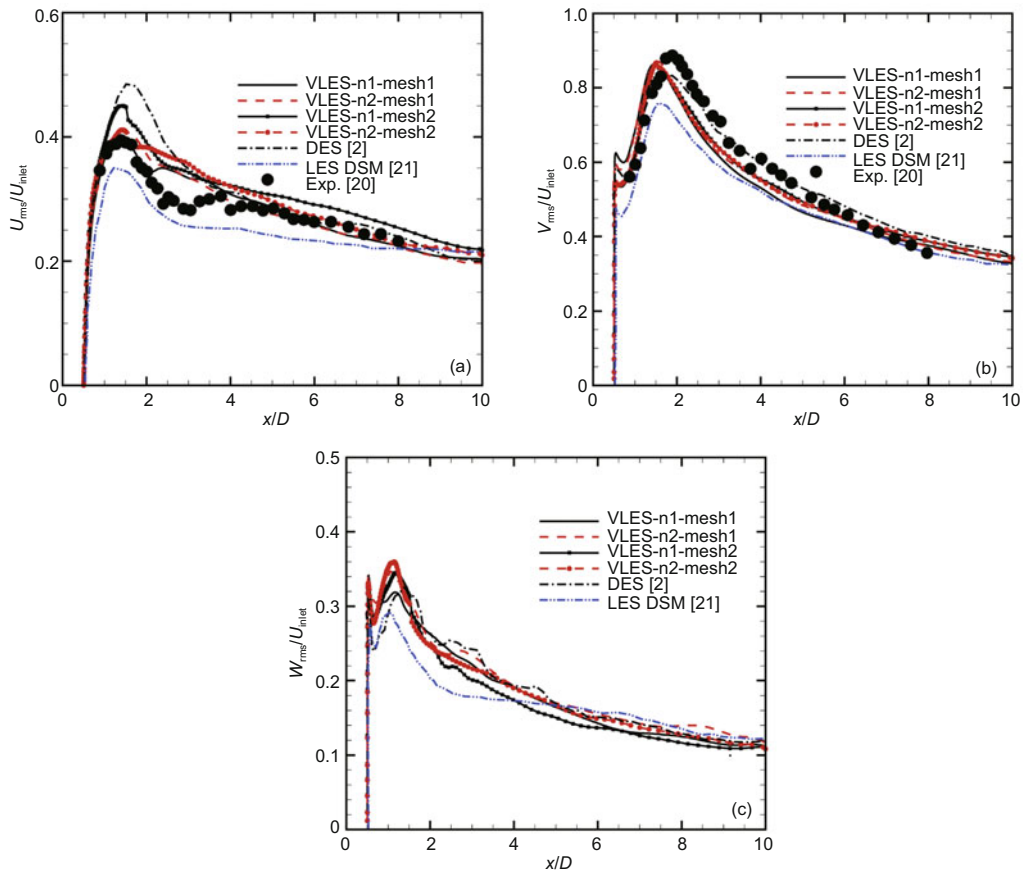


**Figure 5** (Color online) Comparisons of averaged RMS velocities along the central line in the middle plane. (a) RMS velocity in the  $x$  direction; (b) RMS velocity in the  $y$  direction; (c) RMS velocity in the  $z$  direction.

previous results of LES model and DES model. As can be seen from the contours of the RMS flow fields in Figure 4, the RMS velocity distribution along the central line is an index of their individual flow structures. Thus, the shape of the profile in Figure 5 is more important than the value when the predictions are compared with experimental data. From this point of view, the comparisons of RMS streamwise velocity demonstrate that VLES-n1 model performs better than VLES-n2 model as the latter model doesn't predict an obvious peak of the RMS streamwise velocity around the location  $x/D = 1.5$ . With increasing the mesh resolution, the prediction of RMS streamwise velocity by VLES-n1 model is improved, while the VLES-n2 doesn't exhibit the improvement of the prediction. Due to the RMS transverse velocity, the four simulations give close results. Note that the RMS velocity in the transverse direction is much larger than in the streamwise and spanwise directions. This means that these two VLES models are comparative to predict the "very large" flow structures, while due to the relative "small" flow structures, the VLES-n1 model performs better than the VLES-n2 model. This also corresponds to the observations in the channel flow simulation. For the RMS spanwise velocity, the VLES models predict close results compared with DES study in ref. [2]. Overall, present VLES models give better results

than the results by LES dynamics Smagorinsky model in ref. [21] even on the coarse mesh for all the three RMS velocities.

The mean velocity predictions at  $x/D = 1.0$  are shown in Figure 7. The four simulations predict close results, and agree with experimental data well. With increasing the mesh resolution, the results get better for both the two VLES models,

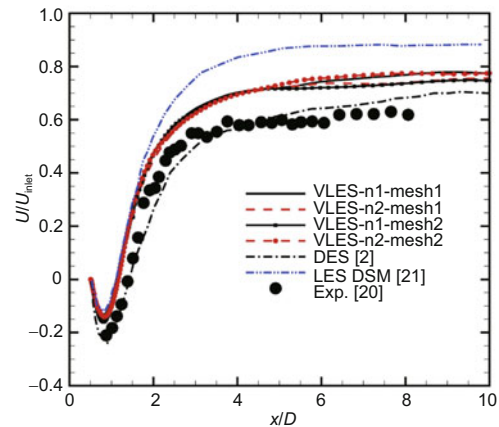


**Figure 6** (Color online) Comparisons of averaged streamwise velocity  $U$  along the central line in the middle plane.

and the VLES-n1 model also performs better on the second set of mesh. For the transverse mean velocity, present VLES models give better results than the DES model.

The comparisons of the velocity profiles at different locations confirm that the present VLES model can efficiently resolve the flow structures for the flow past a square cylinder and the results are generally better than previous LES results. Considering the meshes used here are less than half of those used in previous LES study in ref. [21], it demonstrates the present VLES model is quite efficient and robust for this kind of bluff body flow problems.

The efficient and robust performance of present VLES model is contributed from the reasonable and efficient formulation of the resolution control function  $F_r$  shown in eq. (2). The contours of  $F_r$  in the middle plane by VLES-n1 model are shown in Figure 8. As the grid length is involved in the formulation of  $F_r$ , the contours show this relationship obviously. It can be seen that the  $F_r$  has a value smaller than 0.9 in most of the regions. With increasing the mesh resolution, the value becomes smaller, which can be seen more clearly in the region around the square cylinder (refer to sub Figure (c)). This actually means that less Reynolds stresses need to

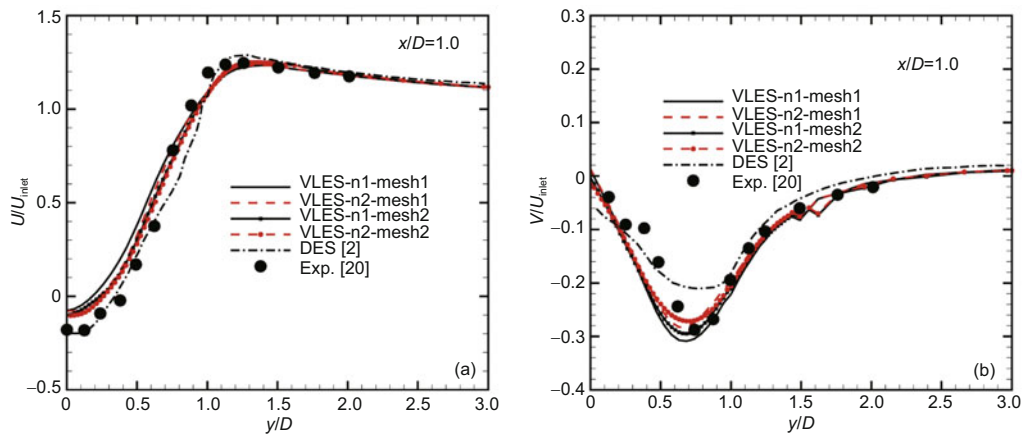


Figure 7 (Color online) Comparisons of the averaged velocity at the location  $x/D = 1.0$  in the middle plane. (a) streamwise velocity  $U$  and (b) transverse velocity  $V$ .

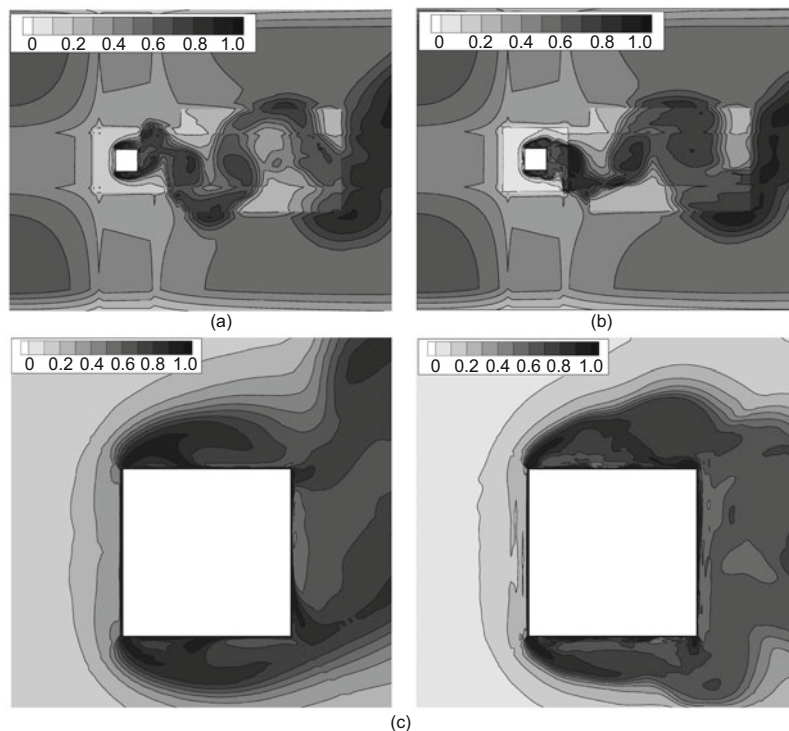


Figure 8 Contours of the resolution control function  $F_r$  in the middle plane. (a) VLES-n1 model on mesh1; (b) VLES-n1 model on mesh2; (c) zoom in the region around the square cylinder.

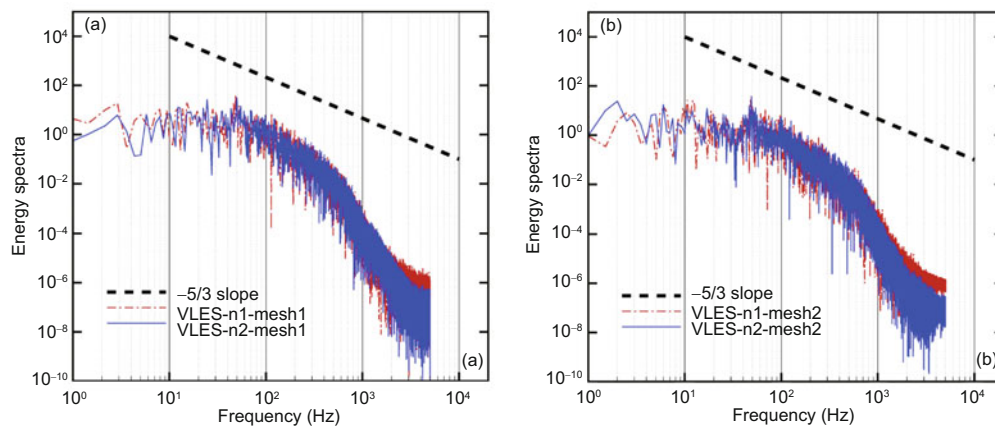
be modelled when the mesh becomes finer, which is the basic concept of VLES methodology. Another feature which should be noted is that the present VLES model can recover to the RANS model near the wall. This is because near the wall, the turbulent integral length scale is very small, thus  $F_r$  approaches the value of 1.0, and then the VLES approaches a RANS simulation. The contours in Figure 8 clearly show that  $F_r$  has a value very close to 1.0 near the wall (refer to the sub figure (c)). This feature is very similar to the DES method. However, the two methods of present VLES model and DES model are different in that away from the wall, DES method runs as a LES mode, while present VLES model runs as a VLES mode. Thus, present VLES model has the advantage that when the local mesh is not fine enough for a LES mode, it can provide a proper mode between the RANS and LES modes, namely, VLES mode, and consequently can be used on a wider range of mesh resolution compared with the DES method.

Figure 9 shows the energy spectrum obtained from present VLES models for the transverse velocity at the location  $(x/D, y/D, z/D) = (2.0, 0, 0)$  on the two meshes. According to the Kolmogorov theory, the energy spectrum of a high Reynolds number flow normally exhibits a  $-5/3$  slope in the inertial subrange. It can be seen that the energy spectrum exhibits an inertial subrange spanning about one decade in the frequency range from about 40 Hz to about 400 Hz. Note that the dominant frequency of the vortex shedding in this flow is around 26 Hz. The results imply that the present VLES model can efficiently resolve most of the energy in the turbulent flow. Besides, the energy spectrum on the first coarse mesh drops off more quickly compared with the one on the second mesh, which means that the present VLES approaches an LES mode with increasing the mesh resolution. Furthermore, the results also demonstrate that the predictions of the VLES-n1 model drop off less quickly than the VLES-n2 model, especially in the region with the high frequency (larger than 1000 Hz), and thus the VLES-n1 model is slightly better than the VLES-n2 model, which is also observed in previous sections.

## 5 Conclusions

In summary, a new unified hybrid turbulence simulation approach, namely VLES method, was proposed in the present study, with a newly proposed resolution control function form for  $F_r$ . The model constants were calibrated in accordance with other hybrid methods. Two different values of  $n$  in  $F_r$  are proposed. Based on Wilcox's  $k-\omega$  turbulence model, the new VLES method was established completely. It was evaluated for two different kinds of flow problems, fully developed turbulent channel flow at  $Re_\tau = 395$  and turbulent flow past a square cylinder at  $Re = 22000$ . For the simulation of channel flow, the present VLES models predict the streamwise mean velocity well on the coarse mesh, and also the near-wall anisotropy in the RMS velocities are captured reasonably. The results are better than those by the Smagorinsky LES model obviously. For the flow past a square cylinder, simulations were performed on two different meshes in order to investigate the efficiency of the present VLES model. It was found that the VLES model can efficiently capture the flow structures such as the vortex shedding, even on a quite coarse mesh compared with previous LES and DES studies. It can give comparable results to that of the Smagorinsky LES model with less than half of the meshes in the simulations, and actually obvious better results are obtained in this flow problem by present VLES models.

Results of both test problems suggest the new VLES method is quite efficient to resolve large flow structures, and its predictive performance is comparable or even superior to that of the Smagorinsky LES model, qualitatively and quantitatively. It can be used for a wide range of mesh resolutions due to the introduction of VLES concept. The form of the resolution control function  $F_r$  shown in eq. (2) is reasonable and efficient for the VLES modeling. The model with a model constant of  $n = 4/3$  shows better performance than with  $n = 2$  and is recommended for further applications. Furthermore, the present VLES model can recover to a RANS simulation near the wall, which can benefit the application



**Figure 9** (Color online) Time energy spectra obtained by VLES models for the transverse velocity at  $(x/D, y/D, z/D) = (2.0, 0, 0)$ . (a) On mesh1; (b) on mesh2.

for other more complex turbulent flows at the high Reynolds number, which are always encountered in a wide range of engineering fluid flow problems.

*This work was supported by the National Natural Science Foundation of China (Grant No. 50936005) and the National Basic Research Program of China (Grant No. 2010CB227302).*

- 1 Spalart P R. Detached-Eddy Simulation. *Annu Rev Fluid Mech*, 2009, 41: 181–202
- 2 Barone M F, Roy C J. Evaluation of Detached Eddy Simulation for turbulent wake applications. *AIAA J*, 2006, 44: 3062–3071
- 3 Forrest J S, Owena I. An investigation of ship airwakes using Detached-Eddy Simulation. *Comput Fluids*, 2010, 39: 656–673
- 4 Escauriaza C, Sotiropoulos F. Lagrangian model of bed-load transport in turbulent junction flows. *J Fluid Mech*, 2011, 666: 36–76
- 5 Huang J B, Xiao Z X, Liu J, et al. Simulation of shock wave buffet and its suppression on an OAT15A supercritical airfoil by IDDES. *Sci China-Phys Mech Astron*, 2012, 55: 260–271
- 6 Speziale C G. Turbulence modeling for time-dependent RANS and VLES: A review. *AIAA J*, 1998, 36: 173–184
- 7 Fasel H F, Seidel J, Wernz S. A methodology for simulations of complex turbulent flows. *J Fluids Eng*, 2002, 124: 933–942
- 8 Zhang H L, Bachman C R, Fasel H F. Application of a new methodology for simulations of complex turbulent flows. *AIAA-2000-2535*
- 9 Sagaut P, Deck S, Terracol M. Multiscale and multiresolution approaches in turbulence. London: Imperial college press, 2006. 244–249
- 10 Han X S. Turbulence modeling for supersonic combustion. Dissertation for the Doctoral Degree. Hefei: University of Science and Technology of China, 2009. 29–50
- 11 Batten P, Goldberg U, Chakravarthy S. Interfacing statistical turbulence closures with large eddy simulation. *AIAA J*, 2004, 42: 485–492
- 12 Liu N S, Shih T H. Turbulence modeling for very large eddy simulation. *AIAA J*, 2006, 44: 687–697
- 13 Hsieh K J, Lien F S, Yee E. Towards a uniformed turbulence simulation approach for wall bounded flows. *Flow Turbulence Combust*, 2010, 84: 193–218
- 14 Peltier L J, Zajaczkowski F J. Maintenance of the near-wall cycle of turbulence for hybrid RANS/LES of fully-developed channel flow. In: 3rd AFOSR International Conference on Direct Numerical Simulation and Large-Eddy Simulation. Kluwer Academic, 2001
- 15 Johansen S T, Wu J Y, Shyy W. Filter-based unsteady RANS computations. *Int J Heat Fluid Flow*, 2004, 25: 10–21
- 16 Wilcox D C. *Turbulence Modeling for CFD*. 2nd ed. La Canada CA: DCW Industries Inc., 1998
- 17 Moser R D, Kim J, Mansour N N. Direct numerical simulation of turbulent channel flow up to  $Re_\tau = 590$ . *Phys Fluids*, 1999, 11: 943–945
- 18 Ma J M, Peng S H, Davidson L, et al. A low Reynolds number variant of partially-averaged Navier-Stokes model for turbulence. *Int J Heat Fluid Flow*, 2011, 32: 652–669
- 19 Smagorinsky J. General circulation experiments with the primitive equations I. The basic experiment. *Month Wea Rev*, 1963, 91: 99–164
- 20 Lyn D A, Einav S, Rodi W, et al. A laser-Doppler velocimetry study of ensemble-averaged characteristics of the turbulent near wake of a square cylinder. *J Fluid Mech*, 1995, 304: 285–319
- 21 Sohankar A, Davidson L. Large eddy simulation of flow past a square cylinder: Comparison of different subgrid scale models. *J Fluids Eng*, 2000, 122: 39–47
- 22 Durao D F G, Heitor M V, Pereira J C F. Measurements of turbulent and periodic flows around a square cross section cylinder. *Exp Fluids*, 1988, 6: 298–304
- 23 Luo S C, Yazdani M G, Chew Y T, et al. Effects of incidence and afterbody shape on flow past bluff cylinders. *J Wind Eng Ind Aerodyn*, 1994, 53: 375–399